Child's Nervous System (2019) 35:823–831
https://doi.org/10.1007/s00381-019-04099-y

ORIGINAL ARTICLE

Panobinostat, a histone deacetylase inhibitor, rescues the angiogenic potential of endothelial colony-forming cells in moyamoya disease

Anshika Jangra[1,2] · Seung Ah Choi[1,2] · Eun Jung Koh[1,2] · Youn Joo Moon[1,2] · Kyu-Chang Wang[1,2] · Ji Hoon Phi[1,2] · Ji Yeoun Lee[1,2,3] · Seung-Ki Kim[1,2]

Received: 5 December 2018 / Accepted: 18 February 2019 / Published online: 27 February 2019

Abstract

Purpose Moyamoya disease (MMD) is one of the most common causes of pediatric stroke. We found defective angiogenic function and downregulation of retinaldehyde dehydrogenase 2 (RALDH2) in MMD endothelial colony-forming cells (ECFCs). Downregulation of RALDH2 mRNA was caused by decreased binding of acetyl-histone H3 (Ac-H3) to the RALDH2 promoter. In this study, we evaluated the feasibility of using a histone deacetylase (HDAC) inhibitor, panobinostat, to upregulate RALDH2 expression and restore the angiogenic potential of MMD ECFCs.

Methods ECFCs from healthy normal controls and patients with MMD were isolated and characterized. After panobinostat treatment, western blot, tube formation, and chromatin immunoprecipitation (ChIP) assays were conducted in vitro. A matrigel plug assay was performed in vivo.

Results Panobinostat increased the levels of Ac-H3 and Ac-H4 in both normal and MMD ECFCs but was much more effective in MMD ECFCs. Increased expression of RALDH2 by panobinostat was observed only in MMD ECFCs. Panobinostat increased the tube formation of both normal and MMD ECFCs in vitro and in vivo, but the effect was greater with MMD ECFCs.

Conclusions We demonstrated that panobinostat increases the angiogenic ability of MMD ECFCs by regulating RALDH2 acetylation. Our results suggest that panobinostat might be a potent therapeutic option for MMD patients.

Keywords Moyamoya disease · Endothelial colony-forming cells · HDAC inhibitor

Introduction

Moyamoya disease (MMD) is a cerebrovascular disorder characterized by progressive stenosis or occlusion of the major bilateral intracranial arteries [1–3]. The predominant feature of this disease is the increased arteriogenesis and angiogenesis, which are considered to lead to progressive ischemia [4, 5]. Endothelial colony-forming cells (ECFCs) have been considered important prerequisites in the pathogenesis of MMD [4, 6, 7]. The cell number and functioning of ECFCs were observed to decrease in pediatric MMD patients [6, 7]. To determine the causes of this phenomenon, we previously analyzed the gene expression profiles of MMD ECFCs compared with normal ECFCs. We found that retinaldehyde dehydrogenase 2 (RALDH2) is downregulated in MMD ECFCs and that the epigenetic suppression of RALDH2 contributed to the defective functioning of these cells [7]. These findings further emphasize the importance of epigenetic changes and the role of genetic modifications within ECFCs.

Previous studies used a histone deacetylase (HDAC) inhibitor to regulate the epigenetic state of ECFCs [8, 9]. Treatment with an HDAC inhibitor increased ECFC-mediated vascular repair in hindlimb ischemia [9, 10], providing a proof of principle that priming ECFCs with epigenetic drugs prior to transplantation is a valuable strategy to improve their regenerative function [8, 9]. A recent report indicated that panobinostat (Farydak®, LBH589), an epigenetic drug [11, 12], accelerates vasculogenesis and blood flow recovery by transplanted

Anshika Jangra and Seung Ah Choi contributed equally to this work.

✉ Seung-Ki Kim
nsthomas@snu.ac.kr

[1] Division of Pediatric Neurosurgery, Seoul Pediatric Clinical Neuroscience Center, Seoul National University Children's Hospital, 101 Daehak-ro, Jongno-gu, Seoul 110-744, Republic of Korea

[2] Department of Neurosurgery, Seoul National University Hospital, Seoul National University College of Medicine, Seoul, South Korea

[3] Department of Anatomy, Seoul National University College of Medicine, Seoul, South Korea

ECFCs in a mouse model of hindlimb ischemia [9]. Panobinostat is a US Food and Drug Administration (FDA)-approved drug that can cross the blood-brain barrier in tissue distribution studies [13] and shows potent inhibitory activity at low concentrations against class I, II, or IV purified HDAC enzymes [14–17].

In this study, we postulated that panobinostat can increase the expression of RALDH2 through the modulation of Ac-H3 and rescue the angiogenic potential of MMD ECFCs.

Materials and methods

ECFC cultures

Blood samples from MMD patients ($N = 5$) and healthy controls ($N = 5$) were obtained (Table 1) with informed consent under the Institutional Review Board (IRB) of the Seoul National University Hospital (SNUH IRB approval number 1610-108-801). The procedures for buffy coat preparation and culture of mononuclear cells (MNCs) for the formation of an ECFC lineage were described in our previous paper [7]. All blood samples (40 ml per sample) were processed within 2 h of collection. The MNCs were plated on precoated culture dishes (collagen type I coating, BD Biosciences, Mountain View, CA) in endothelial cell growth medium (ECGM, PromoCell, Heidelberg, Germany) supplemented with growth factors. The late ECFCs with typical endothelial cobblestone morphology were analyzed by flow cytometry using surface markers, such as CD31, CD34, KDR, CD14, and CD45 [7]. Isolated and cultured ECFCs were used after characterization of the morphology and cell surface markers (Table 2). All cell cultures were maintained in an incubator set to 37 °C with 5% CO_2 in a humidified atmosphere. All experiments, were performed using ECFCs from passage number 8.

Table 1 The information of ECFCs from MMD and normal patients

ECFCs	Sex	Age	RNF231 variant
Normal ECFCs-1	M	24	G/G (wild type)
Normal ECFCs-2	M	24	G/G (wild type)
Normal ECFCs-3	F	26	G/G (wild type)
Normal ECFCs-4	F	26	G/G (wild type)
Normal ECFCs-5	F	27	G/G (wild type)
MMD ECFCs-1	M	6	G/A (heterozygote)
MMD ECFCs-2	F	4	G/G (wild type)
MMD ECFCs-3	F	7	G/G (wild type)
MMD ECFCs-4	M	9	G/A (heterozygote)
MMD ECFCs-5	M	9	G/A (heterozygote)

ECFCs endothelial colony forming cells, *MMD* moyamoya disease

Table 2 The percentages of surface markers in ECFCs

Markers	Normal ECFCs	MMD ECFCs
CD31	99.65 ± 0.38	99.19 ± 0.63
CD34	26.27 ± 20.76	16.77 ± 9.75
KDR	84.02 ± 3.67	78.10 ± 10.35
CD14	2.41 ± 0.62	1.17 ± 0.70
CD45	2.23 ± 1.59	0.90 ± 0.86

ECFCs endothelial colony forming cells, *MMD* moyamoya disease, *CD31* cluster of differentiation 31, *CD34* cluster of differentiation 34, *KDR* kinase insert domain receptor, *CD14* cluster of differentiation 14, *CD45* cluster of differentiation 45

Cell viability assay

The cell growth of normal and MMD ECFCs was assessed by EZ-cytox (DAEIL Lab, Seoul, Korea) according to the manufacturer's protocol. Stock solutions of panobinostat (Selleckchem, Houston, USA) were prepared in DMSO. The cells (4×10^3) were seeded into a 96-well microtiter plate with 100 μl of ECGM per well and incubated for 24 h. The cells were exposed to panobinostat (0–100 nM final concentration) at 48 and 72 h. The cell viability was measured at 450 nm using a spectrophotometer. The results are presented as the percentage of cell viability in treated cells compared with untreated control cells. The IC_{10} (10% inhibitory concentration) and IC_{50} (50% inhibitory concentration) values were calculated using GraphPad Software [18].

Tube formation assay in vitro

Normal and MMD ECFCs (1×10^5 cells) were seeded in a 6-well plate. After 24 h, panobinostat was added to the cells at doses of 0, 2, 4, 6, and 8 nM concentration (as determined via IC_{10} calculations). The cells were plated on a prechilled 48-well cell culture plate coated with 50 μl of unpolymerized Matrigel (Corning, MA) and incubated at 37 °C for 30–45 mins. The cells were then harvested and resuspended in ECGM, (without supplements) containing only 1% fetal bovine serum (FBS, Invitrogen). The cells (2×10^4) were added in triplicate to a 48-well coated plate. After 24 h, the cells were visualized using an inverted microscope (Leica Microsystems GmbH, Wetzlar, Germany) and photographed. Tube formation was analyzed by counting the numbers using ImageJ software, and the data obtained represent the mean of the results.

Western blot analysis

ECFCs were treated with panobinostat for 24 h and 48 h. The primary antibodies used for this experiment were anti-histone H3 (acetyl K27, 1:1000) (Abcam, Cambridge, UK), anti-

histone H4 (acetyl K5 + K8 + K12 + K16, 1:1000) (Abcam), and anti-ALDH1A2 (RALDH2 gene, 1:500, Santa Cruz Biotechnology, TX, USA). After overnight incubation with the primary antibody, the membranes were extensively washed and then incubated with the secondary antibody [18]. The membrane was developed by adding enhanced chemiluminescence (Invitrogen) reagent. The band intensities on the western blots were visualized on X-ray film and quantified by ImageJ software.

Chromatin immunoprecipitation assay

ChIP assays were performed according to the manufacturer's protocol using an Ac-H3 ChIP assay kit (Millipore, Burlington, MA). Normal and MMD ECFCs were treated with doses of 0, 2, 4, and 6 nM panobinostat for 24 h. DNA samples were sonicated using a Bioruptor sonicator (Cosmo Bio, Tokyo, Japan). Immunoprecipitation was performed with normal rabbit IgG (Santa Cruz Biotechnology, TX, USA) and an acetyl-H3K27 antibody (Abcam). Dynabeads® from Invitrogen were used for protein-antibody interactions. The final DNA elution was performed via a ChIP elution kit from Clontech (Takara Bio, CA, USA).

Total ssDNA was extracted from normal and MMD ECFCs using Clontech Elution Kit. Equal amounts of DNA were subsequently amplified using AccuPower PCR premix (Bioneer, Daejon, Korea) with specific primer sets (RALDH2 region 1: sense 5′-GGAGAGCGCATTCTCTTGGT-3′, antisense 5′-AGTTACTGCCTTTGCCTGCT-3′; RALDH2 region 2: sense 5′-TGTGGCACTTGTCTGGGTTT-3′, antisense 5′-CTGCTGGGAATGCTCACAGA-3′; and glyceraldehyde-3-phosphate dehydrogenase (GAPDH): sense 5′-TACT AGCGGTTTTACGGGCG-3′, antisense 5′- TCGAACAG GAGGAGCAGAGAGCGA-3′). The final amplification products were electrophoresed on 2% agarose gels and quantified. The PCR band density was automatically calculated by ImageJ software using the specified area.

In vivo Matrigel plug assay

For in vivo animal experiments, 7-week-old male BALB/c nude mice were housed under pathogen-free conditions. All animal studies were performed, according to the protocol approved by the Institutional Animal Care and Use Committees (IACUCs) at Seoul National University Hospital (IACUC number: 17-0070-S1A0).

When the ECFCs reached 70–80% confluency, the cells were treated with or without 6 nM panobinostat. After 1 day of incubation, ECFCs were prepared in 400 μl of Matrigel (Corning, MA). Then, the mice were divided randomly into five groups ($N = 3$ in each group) as follows: group 1, only Matrigel; group 2, Matrigel + nontreated normal ECFCs; group 3, Matrigel + panobinostat-treated normal ECFCs; group 4, Matrigel + nontreated MMD ECFCs; and group 5, Matrigel + panobinostat-treated MMD ECFCs. The nude mice were injected subcutaneously with Matrigel. Matrigel without ECFCs injection served as the negative control. The mice were sacrificed at 10 days after Matrigel injection, and the plugs were retrieved for immunofluorescence analysis.

Double immunofluorescence was performed with tissue slides prepared from the Matrigel plugs. The slides were deparaffinized and incubated with antigen retrieval solution, which was described in detail in our previous paper [7]. The anti-human nuclei (1:200, Millipore, Temecula) and anti-human CD31 (1:400, Millipore) antibodies were used as primary antibodies, and anti-goat IgG conjugated to Alexa-488 and Alexa-594 (1:500, Invitrogen) was used as the secondary antibody. After mounting with an anti-fading solution containing 4′,-6-diamidino-2-phenylindole (DAPI, Vector Laboratories, Burlingame, CA), the fluorescence signals of the plugs were acquired by a confocal microscope (Leica Microsystems GmbH). Certain hotspots were identified for each Matrigel plug. The number of human nuclei and CD31 double-positive cells per high-power field was determined for three random fields from three random sections of each plug by two independent observers [19].

Statistical analysis

All values were calculated as the means ± SD or expressed as a percentage ± SD of controls from at least three independent experiments. Statistical analysis was performed by a one-way ANOVA, followed by a multiple comparison procedure with a Tukey's multiple comparison test. Student's t test and the Mann-Whitney test were used to compare continuous variables between two groups. Differences were considered statistically significant at $p < 0.05$. GraphPad Prism software (La Jolla, CA, USA) was used for all the analyses.

Results

Panobinostat shows modest cytotoxicity to ECFCs

Cell viability was measured to evaluate the sensitivity of normal and MMD ECFCs to panobinostat. The IC_{50} and IC_{10} in cells treated with panobinostat were calculated. The IC_{50} in normal and MMD ECFCs was 42.5 ± 4.17 nM and 63.9 ± 28.18 nM, respectively (Table 3). When treating with panobinostat up to 100 nM, the IC_{50} could not be obtained for two cases each of normal and MMD ECFCs. The IC_{10} was 9.8 ± 7.07 nM for normal ECFCs and 9.5 ± 3.72 nM for MMD ECFCs, which resulted in minimum cell death. Panobinostat induced a dose-dependent decrease in cell viability in both normal and MMD ECFCs, as confirmed at 72 h

Table 3 IC_{10} and IC_{50} of panobinostat in ECFCs (nM)

Cell name	IC_{10}	IC_{50}
Normal ECFCs-1	4.33	39.02
Normal ECFCs-2	4.60	41.41
Normal ECFCs-3	5.23	47.14
Normal ECFCs-4	18.96	n/a
Normal ECFCs-5	16.0	n/a
MMD ECFCs-1	10.57	95.18
MMD ECFCs-2	13.48	n/a
MMD ECFCs-3	6.22	56.03
MMD ECFCs-4	12.23	n/a
MMD ECFCs-5	5.0	40.49

ECFCs endothelial colony forming cells, *MMD* moyamoya disease, *IC_{10}* 10% inhibitory concentration, *IC_{50}* the half maximal inhibitory concentration, *n/a* not applicable

(Fig. 1). Based on the IC_{10} values, further experiments were performed with doses from 0 to 10 nM. This range showed the highest levels of acetylation in ECFCs.

Panobinostat upregulates the expression levels of Ac-H3, Ac-H4, and RALDH2 in MMD ECFCs

To determine whether histone acetylation is upregulated in ECFCs, the cells were treated with a dose range of panobinostat from 0 to 8 nM. Ac-H3 increased at 8 nM ($p < 0.05$) in normal ECFCs and at 6 nM ($p < 0.05$) and 8 nM ($p < 0.001$) in MMD ECFCs (Fig. 2a and b). In the case of Ac-H4, both normal (6 nM, $p < 0.01$ and 8 nM, $p < 0.001$) and MMD ECFCs (6 nM, $p < 0.05$ and 8 nM, $p < 0.001$) increased at 6 and 8 nM panobinostat respectively (Fig. 2a and c). Interestingly, we found that the RALDH2 protein expression increased strongly at 4 nM ($p < 0.001$), 6 nM ($p < 0.01$), and 8 nM ($p < 0.001$) panobinostat in MMD ECFCs (Fig. 2a and d). However, the expression of RALDH2 was not significantly affected in normal ECFCs. Collectively, these results demonstrate that panobinostat upregulates Ac-H3 and RALDH2 more effectively in MMD ECFCs than in normal ECFCs.

The RALDH2 promoter is more strongly associated with Ac-H3 in MMD ECFCs compared to normal ECFCs

Our previous study demonstrated that the RALDH2 promoter (ascertained by two primer sets: RALDH2 promoter region 1 and RALDH2 promoter region 2) was associated with Ac-H3 in normal ECFCs, while MMD ECFCs had less Ac-H3 association at the RALDH2 promoter region [7]. Based on this result, the experimental data were further analyzed with the two primer sets. As the concentration of panobinostat increased, the expression levels of the RALDH2 promoter region increased. In normal ECFCs, RALDH2 promoter region 1 had no strong increase in expression levels, whereas there was some significant increase in region 2 only after treatment with 6 nM panobinostat ($p < 0.05$, Fig. 3a). The MMD ECFCs showed a significant increase for region 1 at 4 and 6 nM (all $p < 0.05$), and an increase at RALDH2 promoter region 2 was

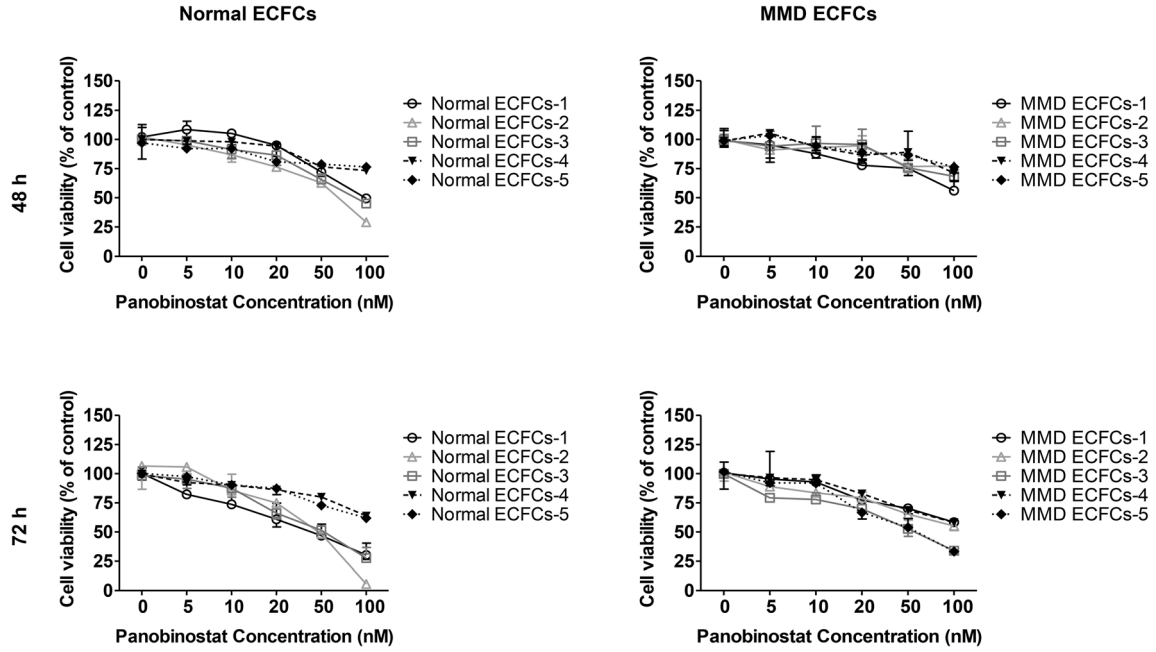

Fig. 1 Dose-response assessment of panobinostat in normal and MMD ECFCs. Cell viability was measured at 48 and 72 h using various concentrations of panobinostat (0–100 nM). The graphs indicate that the cell viability of ECFCs decreased with increasing panobinostat concentration. The IC_{50} and IC_{10} values of panobinostat were 42.5 ± 4.17 and 9.8 ± 7.07 nM in normal ECFCs and 63.9 ± 28.18 and 9.5 ± 3.72 nM in MMD ECFCs

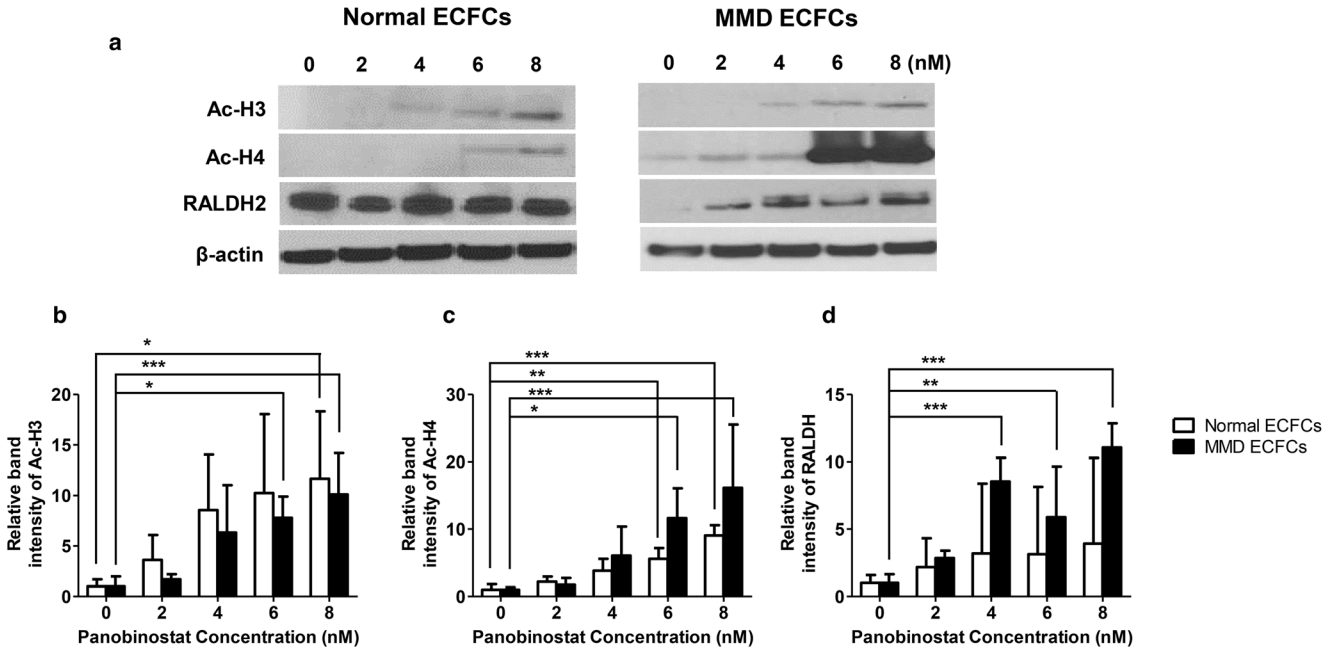

Fig. 2 Panobinostat upregulates the acetylation levels of H3 and H4 and the expression of RALDH2 in ECFCs. **a** Representative immunoblots. **b** Upregulation of Ac-H3 is observed with 8 nM panobinostat in normal ECFCs and with 6 and 8 nM in MMD ECFCs. **c** Ac-H4 was also upregulated in normal and MMD ECFCs after 6 and 8 nM panobinostat treatment. **d** No significant changes were observed for RALDH2 gene expression in normal ECFCs, whereas increasing the dose of panobinostat to 4, 6, and 8 nM increases RALDH2 gene expression in MMD ECFCs. *$p < 0.05$, **$p < 0.01$, ***$p < 0$ .001

detected with 2 nM ($p < 0.05$), 4 nM ($p < 0.01$), and 6 nM ($p < 0.001$) panobinostat (Fig. 3b). As expected, the levels of Ac-H3 and Ac-H4 were significantly enhanced, indicating their binding to the RALDH2 promoter regions 1 and 2 after panobinostat treatment.

Panobinostat stimulates tube formation in MMD ECFCs in vitro

Based on our western blot results showing that panobinostat increased Ac-H3, Ac-H4, and RALDH2 in MMD ECFCs, we

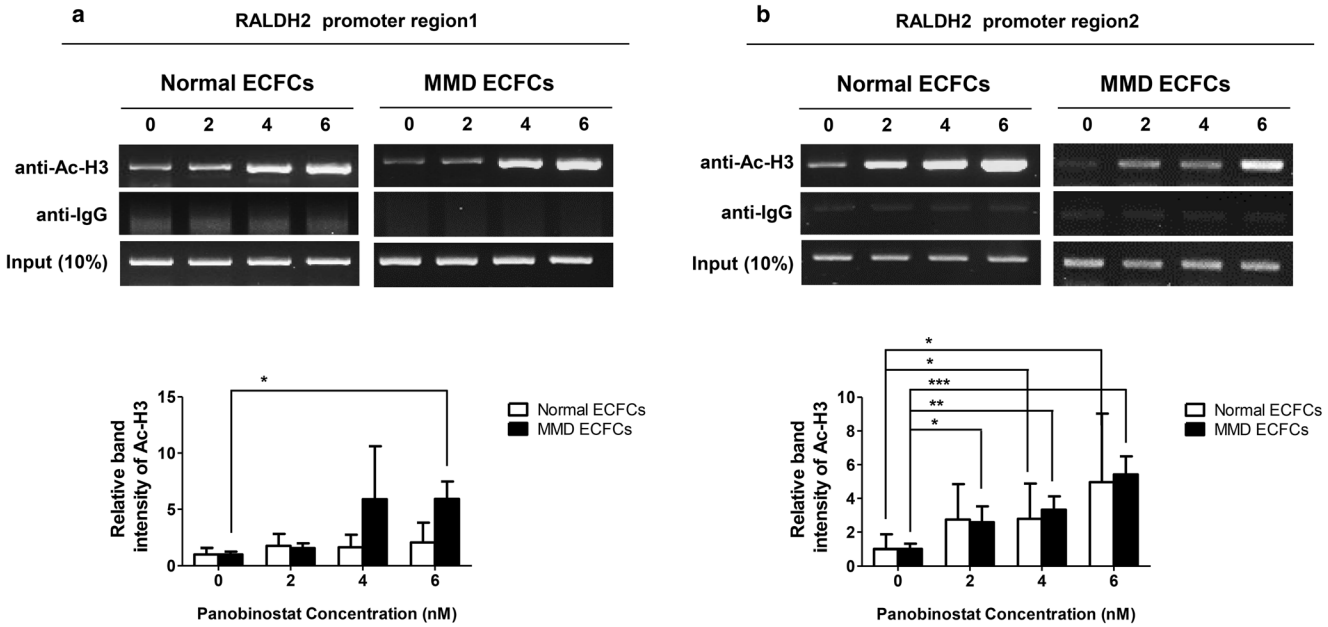

Fig. 3 Panobinostat upregulates the Ac-H3 association at the RALDH2 promoter regions 1 and 2 in MMD ECFCs. **a** In normal ECFCs, the association between Ac-H3 and RALDH2 region 1 was not significant, but an increased pattern is observed in RALDH2 region 2 with 6 nM panobinostat treatment. **b** In MMD ECFCs, an increasing pattern of Ac-H3 is seen in RALDH regions 1 and 2, depending on panobinostat treatment. *$p < 0.05$, **$p < 0.01$, ***$p < 0.001$

speculated that panobinostat could also stimulate the defective tube formation capacity of MMD ECFCs. Therefore, we conducted an in vitro Matrigel tube formation assay in ECFCs. We found that both normal and MMD ECFCs increased tube formation (Fig. 4a and b). Normal ECFCs showed an increase at 4 nM ($p < 0.001$) and 6 nM ($p < 0.01$), but there was no difference at 8 nM panobinostat. MMD ECFCs also showed an increase in tube formation at all doses from 2 to 8 nM (all $p < 0.001$, Fig. 4b). In both normal and MMD ECFCs, the number of tubes was the highest at 6 nM panobinostat, a concentration below the IC_{10}. Interestingly, the rate of increase in MMD ECFCs was much more significant than that in normal ECFCs.

Panobinostat rescues the defective angiogenic potential of MMD ECFCs in vivo

Next, we assessed the angiogenic properties of ECFCs after panobinostat treatment through a Matrigel plug assay in vivo. It is well known that compared to normal ECFCs, MMD ECFCs are abnormal and have defective tube formation ability. After panobinostat treatment, no significant difference was noticed in normal ECFCs (Fig. 5a, $p = 0.5373$), but the number of human nuclei and CD31 co-expressing cells was significantly increased in the panobinostat-treated MMD ECFCs (Fig. 5b, $p < 0.0001$). We verified that the results of the in vivo Matrigel plug assay were consistent with the in vitro tube formation results. These data suggest that panobinostat enhances the angiogenic potential of MMD ECFCs.

Discussion

The present study demonstrated that the HDAC inhibitor panobinostat can increase the expression of RALDH2, which is downregulated in MMD ECFCs, by increasing the acetylation of a histone mark at the RALDH2 promotor region and thus rescue the defective angiogenetic potential of MMD ECFCs. Our previous study reported that RALDH2, the enzyme mediating the biosynthesis of retinoic acid (RA) with a stimulatory effect on angiogenesis, is downregulated in MMD ECFCs, and that the low expression of RALDH2 in MMD

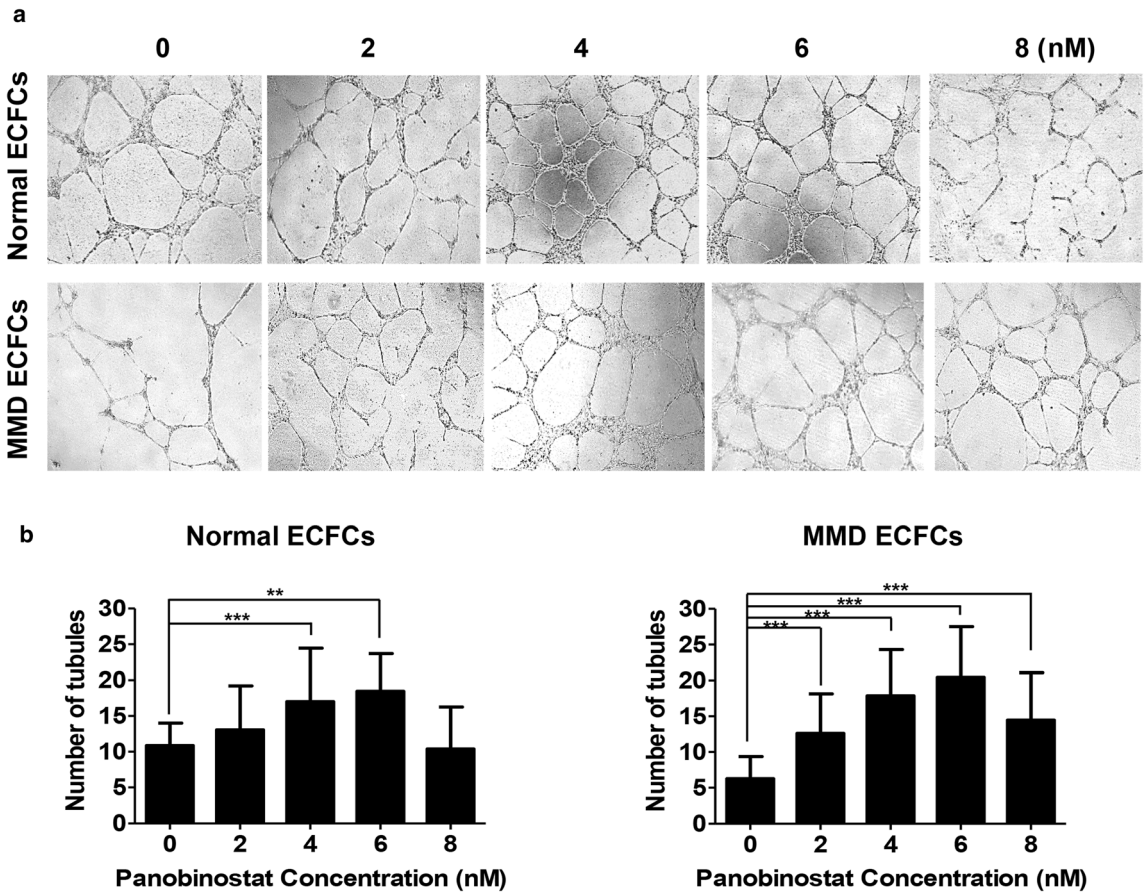

Fig. 4 Panobinostat rescues the angiogenic function of MMD ECFCs in vitro. **a** Representative pictures showing the changes in tube formation of normal and MMD ECFCs after panobinostat treatment. **b** In normal ECFCs, an increase in tube formation is observed with 4 and 6 nM panobinostat, but there was no difference with 2 and 8 nM panobinostat. In MMD ECFCs, tube formation increases at all of the treatment doses of panobinostat, and the maximum tube formation is noticed with 6 nM. *$p < 0.05$, **$p < 0.01$, ***$p < 0.001$

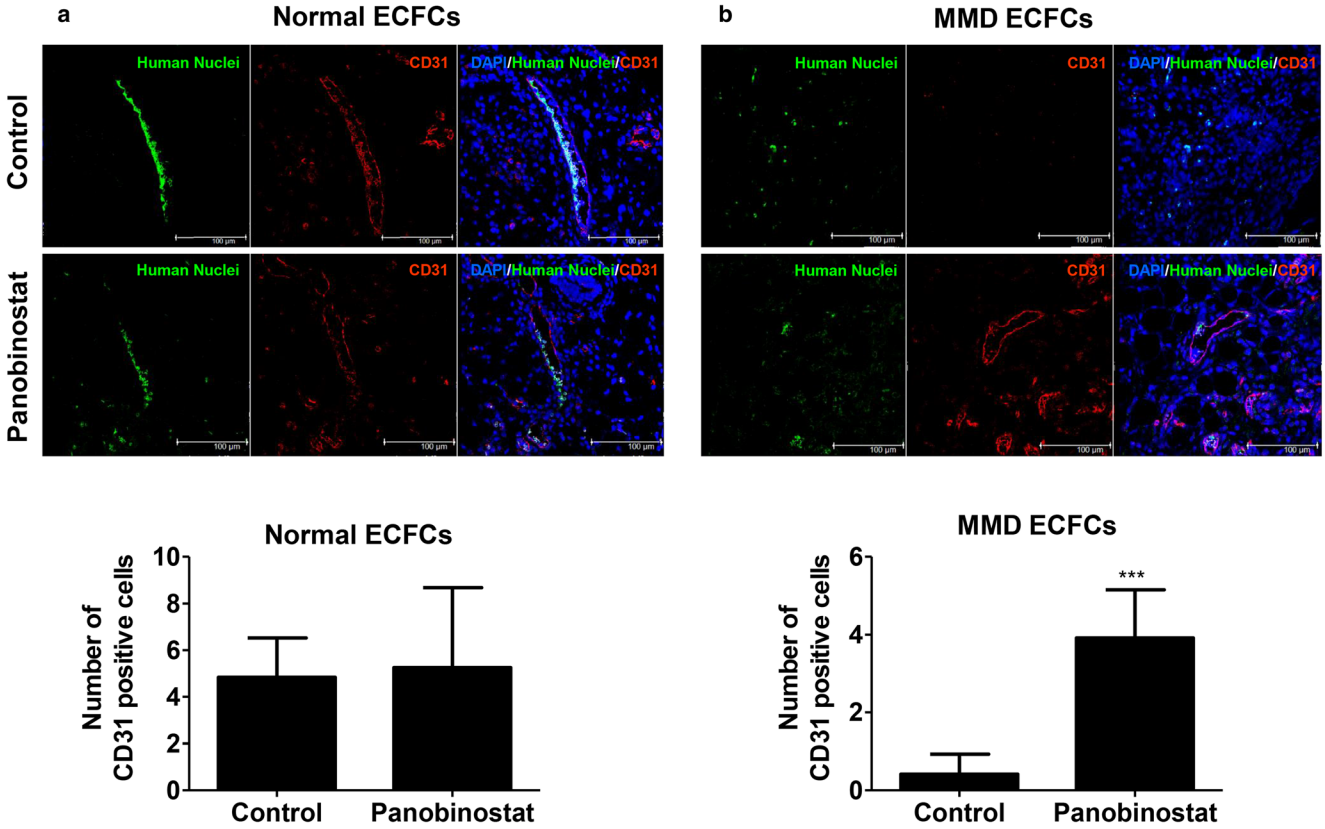

Fig. 5 Panobinostat rescues the angiogenic function of MMD ECFCs in in vivo. Representative pictures of confocal microscopy of cryostat sections of the Matrigel plug containing normal and MMD ECFCs, with or without panobinostat treatment. **a** No significant increase in human nuclei (green) and CD31 (red)-positive cells post panobinostat treatment is discovered in normal ECFCs ($p = 0.5373$). **b** The number of CD31-positive cells is significantly increased in panobinostat-treated MMD ECFCs compared to nontreated MMD ECFCs ($p < 0.0001$). Scale bar for immunofluorescence, 100 μm. Nuclei were counterstained with 4′,6′-diamidino-2-phenylindole (blue). $*p < 0.05$, $**p < 0.01$, $***p < 0.001$

ECFCs is related to the defective acetylation of histone H3K27 [7]. We observed that the tube formation capacity in MMD ECFCs was decreased after the knockdown of RALDH2 in MMD ECFCs, but the angiogenic potential was rescued with all-trans retinoic acid (ATRA) treatment in vitro and in vivo. RALDH2 might be related to the proangiogenic function of ECFCs. Furthermore, it should be noted that the RALDH expression was more sensitive to modulation by Ac-H3 in MMD ECFCs than in normal ECFCs at low concentrations of panobinostat, which did not significantly affect cell survival.

Based on previous research, we hypothesized that [1] histone acetylation at the RALDH2 promotor would be upregulated by treatment with panobinostat, [2] upregulated histone acetylation would lead to increased transcription and expression of RALDH2 [3], and the restoration of RALDH2 expression would rescue the angiogenic potential of MMD ECFCs. The results of the present study, could explain our hypotheses. Panobinostat, increased the expression of Ac-H3 [20, 21], Ac-H4, and RALDH2 in MMD ECFCs. A ChIP assay showed that panobinostat restored histone acetylation at the RALDH2 promotor that was initially lost in MMD ECFCs. Tube formation in MMD ECFCs was increased after panobinostat treatment, as indicated by in vitro and in vivo tube formation assays.

It is known that ECFCs play a crucial role in the pathogenesis of MMD. The cell number and functioning of ECFCs have been found to be decreased or impaired in pediatric MMD patients [9]. We investigated a decrease in the expression level of a certain gene (RALDH2) in MMD ECFCs compared with normal ECFCs, and this difference resulted from epigenetic deregulation. Histone acetylation causes chromatin modifications, resulting in decreased or increased gene transcription. The activity of proteins other than histones is affected by acetylation, and the function of transcription factors can be positively or negatively affected by acetylation. This result provides an explanation about why HDAC inhibition does not always increase the expression of the affected genes even if the chromatin structure is loosened [22].

HDAC inhibitors induce cancer cell cycle arrest, differentiation, and cell death. Moreover, they reduce angiogenesis and modulate the immune response in the cancer microenvironment [22–24]. The anti-angiogenic effects of HDAC inhibitors are associated with the downregulation of proangiogenic

genes, such as the genes for vascular endothelial growth factor (VEGF) [25] or endothelial nitric oxide synthase (eNOS), in endothelial cells [26]. Mottet et al. reported that HDAC7 silencing in endothelial cells altered their morphology and motility and prevented their assembly into tube-like structures in vitro [27]. Moreover, HDAC inhibitors may potentiate both stem-cell differentiation and somatic cell reprogramming [12, 28, 29].

In contrast, some recent studies indicated the proangiogenic property of HDAC inhibitors in ECFCs, similar to our findings. The upregulation of TAL1-dependent genes was due to an increase in histone acetylation by trichostatin A (TSA) [30]. ECFC priming with an HDAC inhibitor, such as TSA, followed by treatment with ECFCs after ischemia increased ECFC-mediated capillary network formation. A follow-up study reported that the combined treatment of ECFCs with the EZH2 inhibitor GSK-343 activates proangiogenic pathways [9]. The authors found that the proangiogenic pathways are repressed in ECFCs due to the presence of bivalent (H3K27me3/H3K4me3 and H3-Ac) epigenetic marks; these marks decrease the regenerative potential of the cells. Treatment using epigenetic drugs led to H3K27me3 removal, H3K4me3 activation, and an increase in H3-Ac; therefore, multiple proangiogenic signaling pathways (VEGFR, CXCR4, WNT, NOTCH, SHH) were activated simultaneously, and the capacity of ECFCs to form capillary networks was improved in vitro and in vivo in a hindlimb ischemia model [8, 9]. The balance between the opposite functions of histone modifications plays an important role in the activation of the pro/anti-angiogenic pathways of ECFCs. Our results suggest that another key mediator of angiogenic functions might be RALDH2 in ECFCs, and the downregulated expression of RALDH2 and the defective angiogenic potential of MMD ECFCs can be improved through histone modification by panobinostat.

From the observations in our study, we suggest that panobinostat could have a certain therapeutic effect in MMD ECFCs. The epigenetic downregulation of RALDH2 expression contributes to the defective angiogenic functioning of MMD ECFCs, and this functioning was targeted via panobinostat. Further study, with an MMD animal model is needed to elucidate the role of panobinostat in rectifying the impaired function of MMD ECFCs.

Funding information This research was supported by a grant from the Korea Health Technology R&D Project through the Korea Health Industry Development Institute (KHIDI), funded by the Ministry of Health & Welfare, Republic of Korea (grant number: HI12C0066).

Compliance with ethical standards Blood samples from MMD patients ($N = 5$) and healthy controls ($N = 5$) were obtained (Table 1) with informed consent under the Institutional Review Board (IRB) of the Seoul National University Hospital (SNUH IRB approval number 1610-108-801).

Conflict of interest The authors have no financial conflicts of interest.

References

1. Kim JS (2016) Moyamoya disease: epidemiology, clinical features, and diagnosis. J Stroke 18:2–11
2. Ismail I, Al-Khafaji K, Mutyala M, Aggarwal S, Al-Khafaji N, Kovacs D, Khosla S, Arora R (2015) "Smoke in the air": a rare cerebrovascular cause of neurological signs and symptoms in a young adult. J Community Hosp Intern Med Perspect 5:27664
3. Ma YG, Zhang Q, Yu LB, Zhao JZ (2016) Role of ring finger protein 213 in moyamoya disease. Chin Med J 129:2497–2501
4. Rafat N, Beck G, Pena-Tapia PG, Schmiedek P, Vajkoczy P (2009) Increased levels of circulating endothelial progenitor cells in patients with moyamoya disease. Stroke 40:432–438
5. Yamashita M, Oka K, Tanaka K (1983) Histopathology of the brain vascular network in moyamoya disease. Stroke 14:50–58
6. Kim JH, Jung JH, Phi JH, Kang HS, Kim JE, Chae JH, Kim SJ, Kim YH, Kim YY, Cho BK, Wang KC, Kim SK (2010) Decreased level and defective function of circulating endothelial progenitor cells in children with moyamoya disease. J Neurosci Res 88:510–518
7. Lee JY, Moon YJ, Lee HO, Park AK, Choi SA, Wang KC, Han JW, Joung JG, Kang HS, Kim JE, Phi JH, Park WY, Kim SK (2015) Deregulation of retinaldehyde dehydrogenase 2 leads to defective angiogenic function of endothelial colony-forming cells in pediatric moyamoya disease. Arterioscler Thromb Vasc Biol 35:1670–1677
8. Fraineau S, Palii CG, Allan DS, Brand M (2015) Epigenetic regulation of endothelial-cell-mediated vascular repair. FEBS J 282:1605–1629
9. Fraineau S, Palii CG, McNeill B, Ritso M, Shelley WC, Prasain N, Chu A, Vion E, Rieck K, Nilufar S, Perkins TJ, Rudnicki MA, Allan DS, Yoder MC, Suuronen EJ, Brand M (2017) Epigenetic activation of pro-angiogenic signaling pathways in human endothelial progenitors increases vasculogenesis. Stem Cell Rep 9:1573–1587
10. Prasain N, Meador JL, Yoder MC (2012) Phenotypic and functional characterization of endothelial colony forming cells derived from human umbilical cord blood. J Vis Exp
11. Atadja P (2009) Development of the pan-DAC inhibitor panobinostat (LBH589): successes and challenges. Cancer Lett 280:233–241
12. Javed MJ, Mead LE, Prater D, Bessler WK, Foster D, Case J, Goebel WS, Yoder MC, Haneline LS, Ingram DA (2008) Endothelial colony forming cells and mesenchymal stem cells are enriched at different gestational ages in human umbilical cord blood. Pediatr Res 64:68–73
13. Seo YJ, Kang Y, Muench L, Reid A, Caesar S, Jean L, Wagner F, Holson E, Haggarty SJ, Weiss P, King P, Carter P, Volkow ND, Fowler JS, Hooker JM, Kim SW (2014) Image-guided synthesis reveals potent blood-brain barrier permeable histone deacetylase inhibitors. ACS Chem Neurosci 5:588–596
14. Fischer A, Sananbenesi F, Mungenast A, Tsai LH (2010) Targeting the correct HDAC(s) to treat cognitive disorders. Trends Pharmacol Sci 31:605–617
15. Qian DZ, Kato Y, Shabbeer S, Wei Y, Verheul HM, Salumbides B, Sanni T, Atadja P, Pili R (2006) Targeting tumor angiogenesis with histone deacetylase inhibitors: the hydroxamic acid derivative LBH589. Clin Cancer Res 12:634–642

16. Gray SG, Ekstrom TJ (2001) The human histone deacetylase family. Exp Cell Res 262:75–83
17. Joshi P, Greco TM, Guise AJ, Luo Y, Yu F, Nesvizhskii AI, Cristea IM (2013) The functional interactome landscape of the human histone deacetylase family. Mol Syst Biol 9:672
18. Lee YE, Choi SA, Kwack PA, Kim HJ, Kim IH, Wang KC, Phi JH, Lee JY, Chong S, Park SH, Park KD, Hwang DW, Joo KM, Kim SK (2017) Repositioning disulfiram as a radiosensitizer against atypical teratoid/rhabdoid tumor. Neuro-Oncology 19:1079–1087
19. Lee C, Lee J, Choi SA, Kim SK, Wang KC, Park SH, Kim SH, Lee JY, Phi JH (2018) M1 macrophage recruitment correlates with worse outcome in SHH medulloblastomas. BMC Cancer 18:535
20. Wang Z, Zang C, Rosenfeld JA, Schones DE, Barski A, Cuddapah S, Cui K, Roh TY, Peng W, Zhang MQ, Zhao K (2008) Combinatorial patterns of histone acetylations and methylations in the human genome. Nat Genet 40:897–903
21. Karlic R, Chung HR, Lasserre J, Vlahovicek K, Vingron M (2010) Histone modification levels are predictive for gene expression. Proc Natl Acad Sci U S A 107:2926–2931
22. Eckschlager T, Plch J, Stiborova M, Hrabeta J (2017) Histone deacetylase inhibitors as anticancer drugs. Int J Mol Sci 18
23. Bolden JE, Peart MJ, Johnstone RW (2006) Anticancer activities of histone deacetylase inhibitors. Nat Rev Drug Discov 5:769–784
24. Kuo MH, Allis CD (1998) Roles of histone acetyltransferases and deacetylases in gene regulation. Bioessays 20:615–626
25. Deroanne CF, Bonjean K, Servotte S, Devy L, Colige A, Clausse N, Blacher S, Verdin E, Foidart JM, Nusgens BV, Castronovo V (2002) Histone deacetylases inhibitors as anti-angiogenic agents altering vascular endothelial growth factor signaling. Oncogene 21:427–436
26. Rossig L, Li H, Fisslthaler B, Urbich C, Fleming I, Forstermann U, Zeiher AM, Dimmeler S (2002) Inhibitors of histone deacetylation downregulate the expression of endothelial nitric oxide synthase and compromise endothelial cell function in vasorelaxation and angiogenesis. Circ Res 91:837–844
27. Mottet D, Bellahcene A, Pirotte S, Waltregny D, Deroanne C, Lamour V, Lidereau R, Castronovo V (2007) Histone deacetylase 7 silencing alters endothelial cell migration, a key step in angiogenesis. Circ Res 101:1237–1246
28. Bapat SA (2013) Epigenetic regulation of cancer stem cell gene expression. Subcell Biochem 61:419–434
29. Bouvard C, Gafsou B, Dizier B, Galy-Fauroux I, Lokajczyk A, Boisson-Vidal C, Fischer AM, Helley D (2010) Alpha6-integrin subunit plays a major role in the proangiogenic properties of endothelial progenitor cells. Arterioscler Thromb Vasc Biol 30:1569–1575
30. Palii CG, Vulesevic B, Fraineau S, Pranckeviciene E, Griffith AJ, Chu A, Faralli H, Li Y, McNeill B, Sun J, Perkins TJ, Dilworth FJ, Perez-Iratxeta C, Suuronen EJ, Allan DS, Brand M (2014) Trichostatin A enhances vascular repair by injected human endothelial progenitors through increasing the expression of TAL1-dependent genes. Cell Stem Cell 14:644–657